Journal of Catalysis **189,** 349–359 (2000)
doi:10.1006/jcat.1999.2684, available online at http://www.idealibrary.com on IDEAL®

# $CO_2$ Reforming of $CH_4$ by Atmospheric Pressure ac Discharge Plasmas

Aimin Huang,* Guanguang Xia,† Jinyun Wang,* Steven L. Suib,[1,*,†,‡]
Yuji Hayashi,§ and Hiroshige Matsumoto¶

*Department of Chemistry, †Institute of Materials Sciences, and ‡Department of Chemical Engineering, University of Connecticut, Storrs, Connecticut 06269; §Fujitsu Laboratories, Ltd., 1015 Kamikodanaka, Nakahara, 211 Japan; and ¶Department of Chemistry, Nakasaki University, Bunkyomachi 1-14, Nakasaki, 852 Japan

Received May 17, 1999; revised September 7, 1999; accepted September 13, 1999

**Partial oxidative reactions of methane by carbon dioxide have been studied using atmospheric pressure alternating current plasmas. The reactions were carried out using a Y-type reactor with metal rods as the inner electrodes inside quartz tubes and aluminum foil wrapped around quartz tubes as the outer electrodes. The waveforms, input voltages, and currents of the reactions were monitored with an oscilloscope. Interactions between excited methane and excited carbon dioxide as well as those between one excited species and the other unexcited species were observed. The products of the reactions include carbon monoxide, hydrogen, ethane, ethylene, propane, and acetylene. The effects of many reaction parameters, including input voltage, total flow rate, mole ratio of methane to carbon dioxide, selective excitation of either reactant, and micro-arc formation, on product distribution and energy efficiency have been investigated. With an increase in the carbon dioxide-to-methane ratio the selectivity to carbon monoxide increased, and less coke formed. Micro-arc formation between excited methane and excited carbon dioxide increased the conversions of both methane and carbon dioxide and favored the production of carbon monoxide. The energy efficiency of the reaction reached a maximum at $CH_4/CO_2 = 1$ with micro-arc formation, but it was minimized at $CH_4/CO_2 = 1$ when no micro-arc formed during the reaction. The reaction with micro-arc formation had a higher energy efficiency than that without micro-arc formation.** 

## INTRODUCTION

Global warming has been a big concern that has attracted the attention of many scientists for many years. Although many greenhouse gases, such as $CO_2$, $NO_x$, and halogenated hydrocarbons, contribute to global warming (1–3), more than half of the warming is caused by the increased concentration of carbon dioxide (4–7), which comes from fossil fuel combustion, a major energy source. Therefore, decreases of emission and environmental friendly utilization of $CO_2$ have become areas of great interest to the world.

Although many efforts have been dedicated to regulate emission (8, 9), the process is slow because of political obstacles and economic concerns in developing countries. Therefore, utilization of fossil fuels will continue to be a major energy source, which will continue to increase $CO_2$ emission (10).

Another direction in reducing $CO_2$ concentration is the remediation of $CO_2$ (11–14), which has become a very vigorously investigated research area. Current interests in $CO_2$ utilization include hydrogenation of $CO_2$ and $CH_4$ catalytic reforming by $CO_2$. Application of the former will be limited because of the high cost of hydrogen. $CH_4$ reforming with $CO_2$ to produce synthesis gas for the synthesis of materials such as acetic acid, dimethyl either, and alcohols by oxoalcohol synthesis (15, 16) may become economically feasible and therefore has become a major focus of researchers.

A lot of research has been done in catalytic reforming of $CH_4$ with $CO_2$. The catalysts reported include metal-oxide-supported noble metals (17–19), Ni-metal oxides (20–22), and Ni-zeolites (23, 24) systems. The catalyst systems, kinetics, and mechanistic studies of this catalytic process were reviewed by Bradford (25). However, these catalytic reactions have several drawbacks, including high temperature and fast coke formation, leading to the deactivation of catalysts.

Plasma processes have been utilized in many chemical reactions, such as $CO_2$ direct decomposition (26), methane oligomerization (27, 28), and decomposition of halogenated hydrocarbons (29, 30). Plasmas have advantages over other processes in realizing thermodynamically unfavorable reactions such as $CH_4 + CO_2 \rightarrow 2CO + 2H_2$, $\Delta H^{\circ}_{298K} =$ 247.0 kJ/mol due to potential nonthermodynamic (local) equilibria. This process also overcomes the drawback of the high temperature required by conventional catalytic processes. In this paper, we present a $CH_4 + CO_2$ reaction process initiated by an alternating current (ac) plasma at atmospheric pressure using a Y-type reactor. The effects of selective excitation of one reactant, the input voltage, reactant concentrations, and the flow rate on reactant conversions and product distributions were investigated. The dependence of energy efficiencies of these reactions on several experimental parameters will also be discussed.

[1] To whom correspondence should be addressed.



0021-9517/00 $35.00

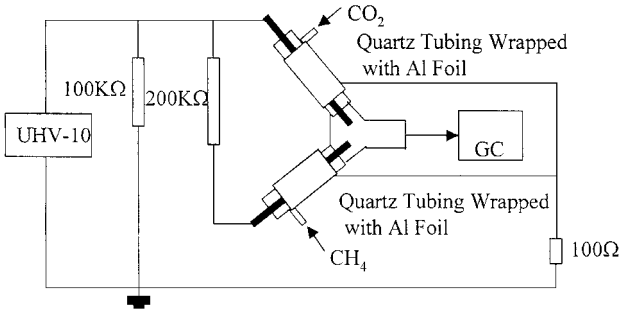


**FIG. 1.** Circuit diagram of the reaction setup.

## EXPERIMENTAL

### Apparatus

The experiments were carried out using a Y-type quartz reactor invented by Xia, who addressed the design detail and characteristics of the reactor elsewhere (31). The circuit diagram for the reaction is shown in Fig. 1 where the angle between the two arms is 120°. The power was generated by a UHV-10 ac electric generator (Nihon Inter Electronics Corp., Japan). An input voltage can be applied on either or both arms of the Y-type reactor to generate plasmas according to reaction specifications. $CO_2$ and $CH_4$ were introduced into these two arms separately for the convenience of selectively activating either reactant. The inner electrodes for the reactor are stainless steel rods with a diameter of 8 mm, and the outer electrodes are aluminum foil wrapped around quartz tubes with 10-mm inner diameters and 12-mm outer diameters. Plasmas were generated between the inner electrodes and the inner walls of the quartz tubes. At certain conditions micro-arcs formed between these two arms. The voltages and currents of the reactions were measured using a high-voltage probe and a low-voltage probe, respectively. The waveforms and measurements of the input voltage and current were monitored closely with a DL-1540 Yokogawa oscilloscope (Yokogawa Electronics Corp., Japan).

### Materials Preparation and Analyses

Ultra pure $CO_2$, $CH_4$ (>99.9%), and He (>99.99%) were obtained from Connecticut Airgas, Inc. Different concentrations of the reactants were prepared from the above gases using a gas-mixing panel. The total carbon concentration was 10%, while the ratio of $CH_4/CO_2$ varied, depending on the reactions.

The reaction products were analyzed with an MKS-UTI PPT quadrupole residual gas analyzer mass spectrometer and an HP 5890A gas chromatograph equipped with a TCD (thermal conductivity detector). The concentrations of $CO_2$ and $CH_4$ were determined by external standard calibrations, while those of CO and other hydrocarbons were calculated based on their relative response factors.

### Calculations

According to the reaction $CH_4 + CO_2 \rightarrow 2CO + 2H_2$, the flow rate changed after the reaction due to a change in moles. An estimation of the flow change for the reaction can be calculated as follows: Assuming 50% conversion for each reactant, 100 ml/min total inlet flow rate, $[CH_4]_i/[CO_2]_i = 1$, and $[CH_4]_i + [CO_2]_i = 10\%$, the flow rate after the reaction will be

$$100 - 50\% \times 10\% \times 100 + 50\% \times 10\% \times 2 = 105.$$

Due to the relatively small deviation due to the flow change and the complexity of the reaction products, we based our calculation on the assumption of a constant flow. Conversions of $CH_4$ and $CO_2$ are defined as follows:

$$X_{CH_4}\% = 100 \times ([CH_4]_i - [CH_4]_o)/[CH_4]_i \quad [1]$$

$$X_{CO_2}\% = 100 \times ([CO_2]_i - [CO_2]_o)/[CO_2]_i \quad [2]$$

Selectivities to CO, $H_2$, $C_2H_6$, $C_2H_4$, $C_3H_8$, and $C_2H_2$, calculated based on the total carbon conversion, are defined as follows,

$$S_{CO}\% = 100 \times [CO]_o/(([CO_2]_i - [CO_2]_o) + ([CH_4]_i - [CH_4]_o)), \quad [3]$$

$$S_{C_2H_6}\% = 100 \times 2 \times [C_2H_6]_o/(([CO_2]_i - [CO_2]_o) + ([CH_4]_i - [CH_4]_o)), \quad [4]$$

$$S_{C_2H_4}\% = 100 \times 2 \times [C_2H_4]_o/(([CO_2]_i - [CO_2]_o) + ([CH_4]_i - [CH_4]_o)), \quad [5]$$

$$S_{C_2H_2}\% = 100 \times 2 \times [C_2H_2]_o/(([CO_2]_i - [CO_2]_o) + ([CH_4]_i - [CH_4]_o)), \quad [6]$$

$$S_{C_3H_8}\% = 100 \times 3 \times [C_3H_8]_o/(([CO_2]_i - [CO_2]_o) + ([CH_4]_i - [CH_4]_o)), \quad [7]$$

$$B_C = S_{CO} + S_{C_2H_6} + S_{C_2H_4} + S_{C_2H_2} + S_{C_3H_8}, \quad [8]$$

where $[CH_4]_i$ and $[CO_2]_i$ are inlet concentrations of $CH_4$ and $CO_2$; $[CH_4]_o$, $[CO_2]_o$, $[C_2H_6]_o$, $[C_2H_4]_o$, $[C_2H_2]_o$, and $[C_3H_8]_o$ are outlet concentrations of $CH_4$, $CO_2$, CO, $C_2H_6$, $C_2H_4$, $C_2H_2$, and $C_3H_8$; $X_{CH_4}$ and $X_{CO_2}$ are conversions of $CH_4$ and $CO_2$; $S_{CO}$, $S_{C_2H_6}$, $S_{C_2H_4}$, $S_{C_2H_2}$, and $S_{C_3H_8}$ are selectivities of CO, $C_2H_6$, $C_2H_4$, $C_2H_2$, and $C_3H_8$. $B_C$ is the carbon balance of the reaction.

The $CO_2$-based selectivity to CO, ${}^*S_{CO}$, is defined as the selectivity based solely on $CO_2$, assuming that all CO was from $CO_2$ decomposition and no CO was from $CH_4$. The calculation for ${}^*S_{CO}$ is as follows:

$$S_{CO} = [CO]_o/([CO_2]_i - [CO_2]_o). \quad [9]$$

The efficiency $\xi$ of the reaction is defined as

$$\xi\% = E_{cal}/E_{exp} \times 100, \quad [10]$$

$$E_{cal} = \sum \Delta H_{f,products} - \sum \Delta H_{f,reactants}, \quad [11]$$

$$E_{exp} = 1/t \int_0^t (V \times I)\, dt, \quad [12]$$

where $\Delta H_{f,\,products}$ and $\Delta H_{f,\,reactants}$ are the heat of formation for all individual products and reactants and $V$ and $I$, measured by an oscilloscope, are the voltage and current applied to the reactor, respectively. $E_{cal}$ includes the theoretical energy consumption for all reactions that occur. $E_{exp}$ is the time average experimental energy consumption, read directly from the oscilloscope, which calculated $E_{exp}$ from $V$ and $I$ using its internal mathematics functions.

## RESULTS

### I. $CH_4$ and $CO_2$ Reactions by Glow Discharge Plasmas

#### 1. $CH_4 + CO_2$ Reaction in the Y-type Reactor with Both $CH_4$ and $CO_2$ Excited

*1.1. Effects of $CH_4/CO_2$ mole ratio.* $CH_4$ and $CO_2$ plasma reactions were carried out in the Y-type reactor. During the reaction, both $CH_4$ and $CO_2$ were excited at an average (root-mean-square, abbreviated as rms) voltage of $V_{rms} = 1.91$ kV. The average current $I_{rms} = 17.4$ mA. Purple discharge plasmas were generated between the inner electrodes and the inner walls of the quartz tubes. Typical voltage and current waveforms are shown in Fig. 2. CO, $H_2$, trace amounts of $H_2O$, and hydrocarbons, including ethane, ethylene, acetylene, and propane, were detected as reaction products. The results are shown in Table 1.

As the $CH_4/CO_2$ mole ratio decreased from 9/1 to 1/9, the conversion of $CH_4$ increased from 34 to 70% while that of $CO_2$ decreased from about 53 to 17%. Selectivities of CO and $H_2$ increased from 28 to 97% and 47.9 to 66.0%, respectively, with a decreasing $CH_4/CO_2$ ratio. Less $C_2$'s and $C_3$'s were formed when $CO_2$ was in excess compared with that when $CH_4$ was in excess. At high $CH_4/CO_2$ ratios, the carbon balance was low because of the formation of coke deposits during the reaction. As the $CH_4/CO_2$ ratio increased, more coke deposits were formed.

**TABLE 1**

**Results of $CH_4 + CO_2$ Reaction with $CH_4$ and $CO_2$ Both Excited**

| $CH_4/CO_2$ (at.) | $X_{CH_4}$ (%) | $X_{CO_2}$ (%) | $S_{CO}$ (%) | $S_{C_2H_6}$ (%) | $S_{C_2H_4}$ (%) | $S_{C_3H_8}$ (%) | $S_{H_2}$ (%) | $B_C$ (%) |
|---|---|---|---|---|---|---|---|---|
| 1/9 | 70.0 | 16.6 | 97.0 | 9.1 | 0.0 | 0.0 | 66.0 | 106 |
| 3/7 | 65.4 | 19.3 | 73.8 | 14.1 | 0.0 | 1.5 | 58.9 | 89.4 |
| 5/5 | 56.8 | 28.5 | 49.0 | 16.7 | 1.4 | 4.2 | 56.0 | 71.3 |
| 7/3 | 45.0 | 39.8 | 36.2 | 21.9 | 1.7 | 6.6 | 53.4 | 66.4 |
| 9/1 | 34.0 | 52.8 | 27.8 | 25.2 | 2.3 | 6.9 | 47.9 | 66.2 |

*Note.* $X_{CH_4}$ (%), conversion of $CH_4$; $X_{CO_2}$ (%), conversion of $CO_2$; $S_{CO}$ (%), selectivity of CO; $S_{C_2H_6}$ (%), selectivity of $C_2H_6$; $S_{C_2H_4}$ (%), selectivity of $C_2H_4$; $S_{H_2}$ (%), selectivity of $H_2$; $B_C$ (%), carbon balance.

*1.2. Effects of flow rate.* The effects of the flow rate on the reactions are shown in Fig. 3. A change in the flow rate did not affect the product distribution for this reaction, although both $CO_2$ and $CH_4$ conversions decreased as the flow rate increased. The reaction rates of $CO_2$ and $CH_4$ and the total carbon reaction rate are computed by using Eqs. [13], [14], and [15], respectively. The dependencies of these reaction rates on the flow rate are shown in Fig. 4. The reaction rates increased with increasing flow rate, although the increase in the $CH_4$ reaction rate was larger than that of $CO_2$. Equations [13]–[15] are used to determine reaction rates as follows:

$$\text{Reaction rate of } CO_2 \text{ (mol/h)} = X_{CO_2} \times [CO_2] \times Q \times 60/24{,}500, \quad [13]$$

$$\text{Reaction rate of } CH_4 \text{ (mol/h)} = X_{CH_4} \times [CH_4] \times Q \times 60/24{,}500, \quad [14]$$

$$\text{Total carbon reaction rate} = \text{Reaction rate of } CO_2 + \text{Reaction rate of } CH_4, \quad [15]$$

where, $X_{CO_2}$, $X_{CH_4}$, $[CO_2]$, and $[CH_4]$ stand for the conversions of $CO_2$ and $CH_4$ and the initial concentrations of $CO_2$ and $CH_4$, respectively. $Q$ is the total flow rate (in ml/min) of the reaction. The number of milliliters in 1 mol of a gas at room temperature is 24,500. The conversion 60 is for expressions in minutes.

*1.3. Effects of input voltage.* As shown in Fig. 5, increasing the input voltage increased the $CO_2$ and $CH_4$ conversions as well as the selectivity to CO. However, more coke deposits formed at a higher input voltage. A high input voltage also favored the formation of higher dehydrogenation products like $C_2H_2$.

#### 2. Reactions with Selective Excitation of $CH_4$ in a Y-type Reactor

The results of $CO_2 + CH_4$ reactions with only $CH_4$ excited at different input voltages are shown in Fig. 6. When the input voltage was applied only to the $CH_4$ arm, plasmas were observed in the $CH_4$ arm, indicating excitation of $CH_4$. Although no plasmas were observed in the $CO_2$ arm, both $CH_4$ and $CO_2$ were converted. The conversions of $CH_4$ and $CO_2$ increased from 16.3 to 41.3% and from 2.2 to 12.1%, respectively, as the input voltage increased from 2.5 to 9 kV. The reaction products included not only $C_2$'s and $C_3$'s, which were the products of $CH_4$ oligomerization, but also CO, indicating the participation of $CO_2$ in the reaction. The selectivity to CO increased from 14.2 to 25.9% as the input voltage increased from 2.5 to 9 kV. These results suggest

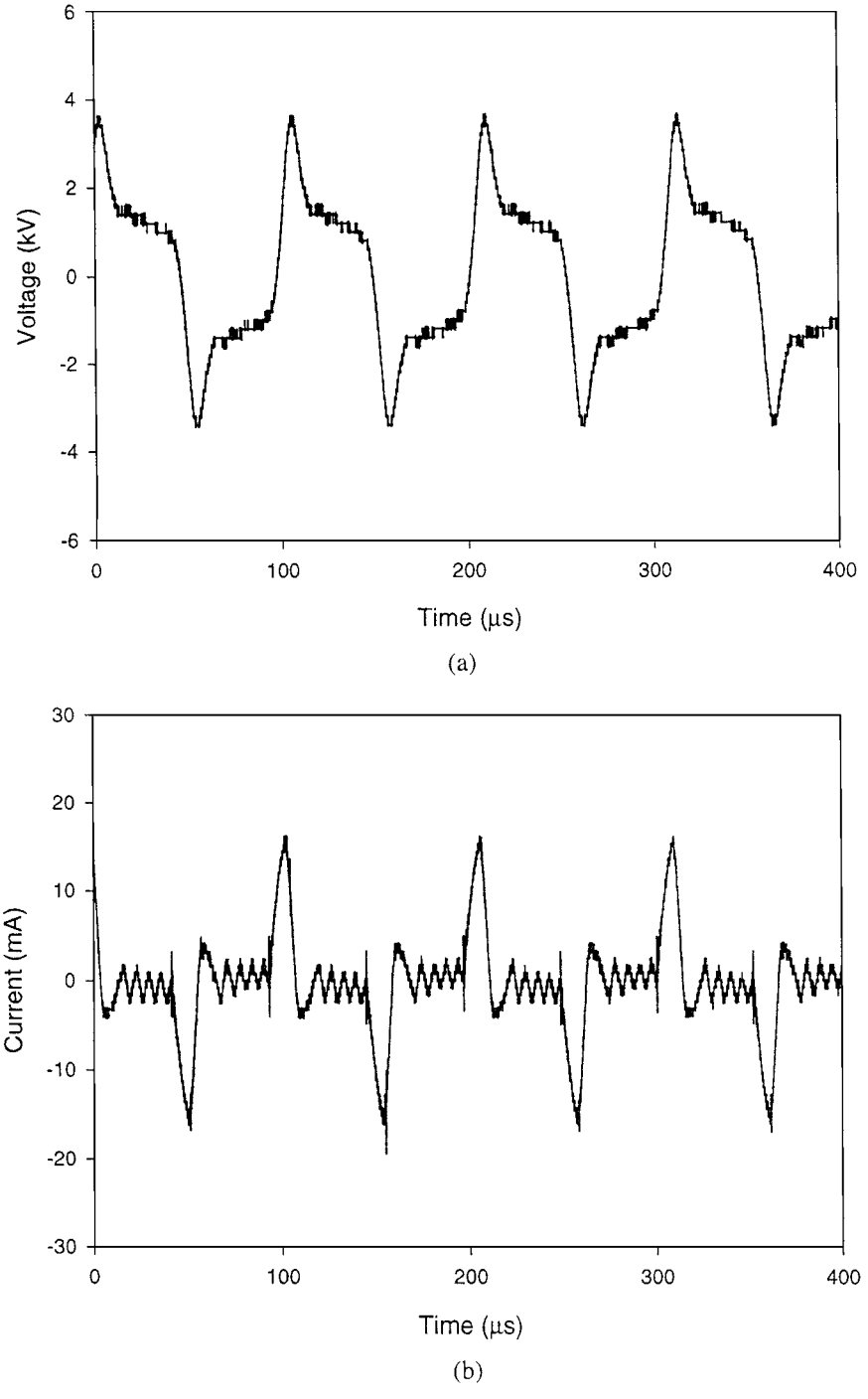


**FIG. 2.** Voltage (a) and current (b) waveforms for the reaction with glow discharge plasmas.

an interaction occurred between excited $CH_4$ or its excited intermediates and unexcited $CO_2$ during these reactions.

### 3. *Reactions with Selective Excitation of $CO_2$ in the Y-type Reactor*

Figure 7 shows the results of partial oxidation of $CH_4$ by excited $CO_2$ at different input voltages. The starting excitation voltage of $CO_2$ was higher than that of $CH_4$ because of higher energy requirements for the excitation of $CO_2$. Plasmas were only observed in the $CO_2$ arm, indicating excitation of $CO_2$. As the input voltage increased, the conversions of $CH_4$ and $CO_2$ both increased, and the selectivity to CO decreased slightly. Besides CO, small amounts of other products, including $C_2H_6$ and $C_2H_4$, were observed, indicating oxidation of $CH_4$ by excited $CO_2$ or its excited intermediates.

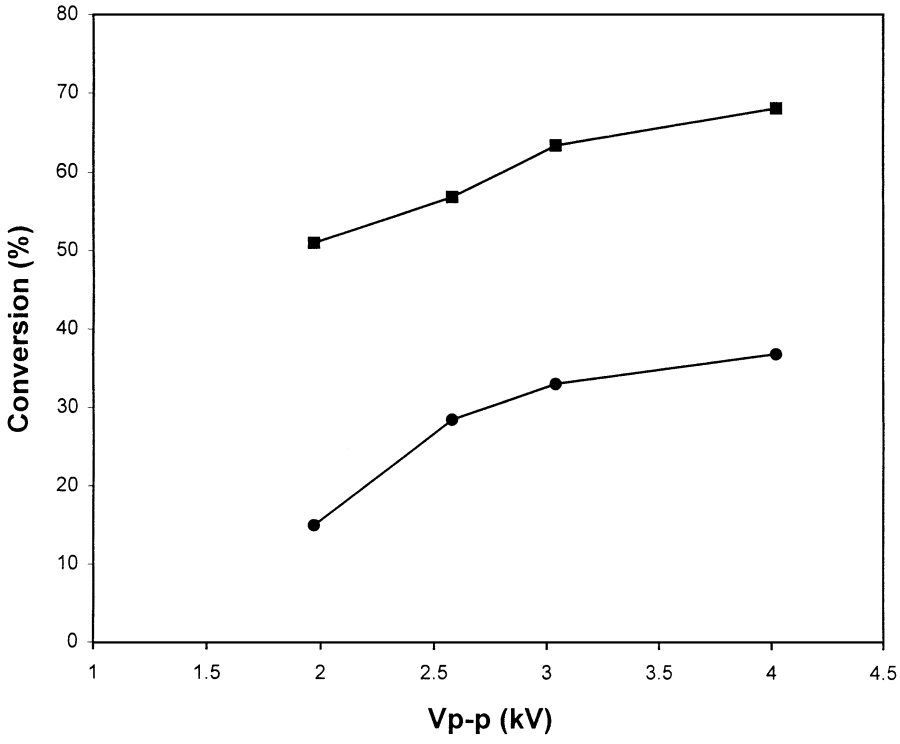


**FIG. 3.** Dependence of $CO_2$ (●) and $CH_4$ (■) conversions on the reaction flow rate. $CH_4/CO_2 = 1$; $V_{rms} = 2.10$ kV; $I_{rms} = 17.4$ mA.

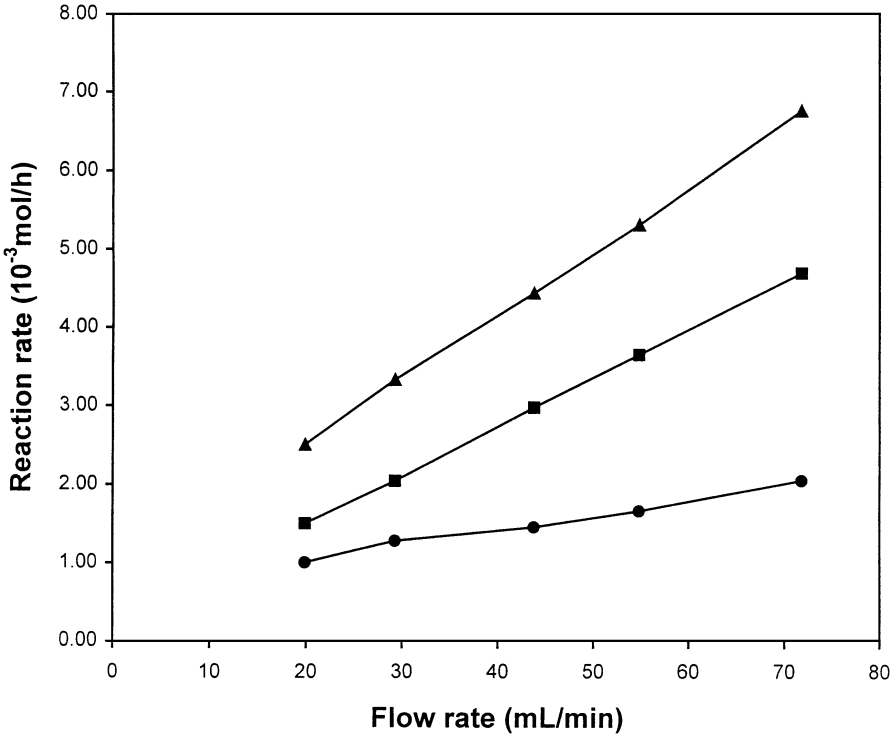


**FIG. 4.** Dependence of reaction rates ($CH_4$ (■), $CO_2$ (●), total (▲)) on flow rate. $CH_4/CO_2 = 1$; $V_{rms} = 2.10$ kV; $I_{rms} = 17.4$ mA.

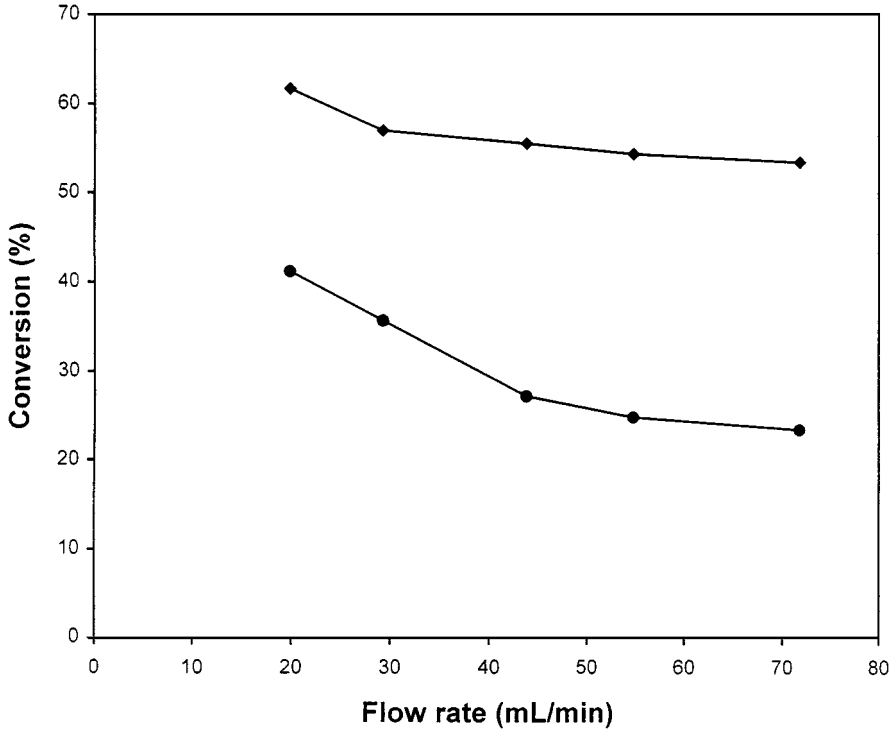


**FIG. 5.** Effects of input voltage on the conversions of $CO_2$ (●) and $CH_4$ (■). $CH_4/CO_2 = 1$; total flow rate = 40 ml/min.

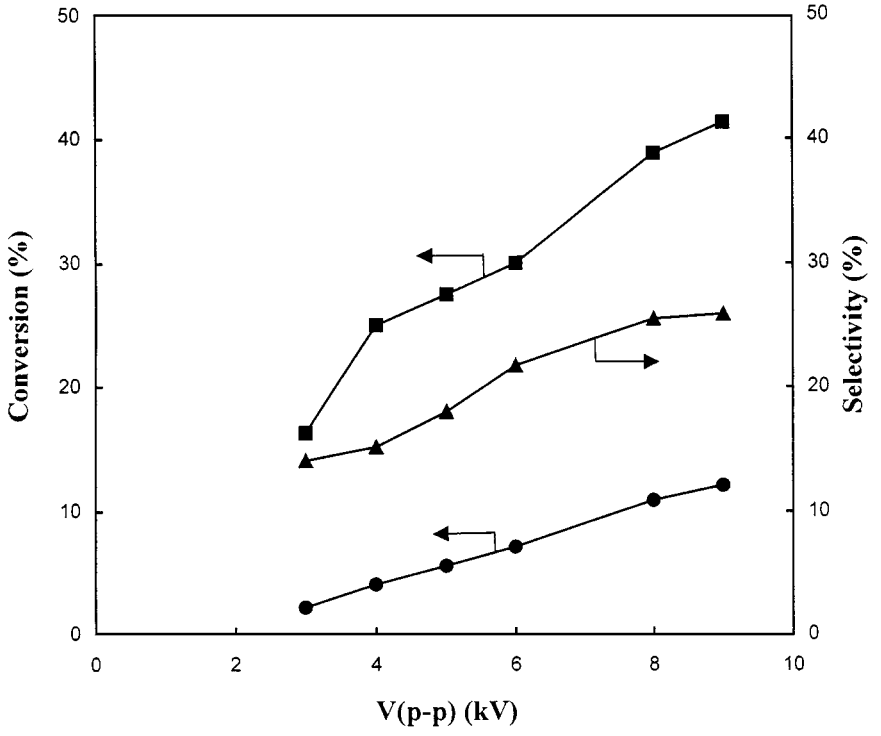


**FIG. 6.** Results of reactions between $CO_2$ and excited $CH_4$. (●) $CO_2$ conversion; (■) $CH_4$ conversion; (▲) CO selectivity; $CH_4/CO_2 = 1$; total flow rate = 40 ml/min.

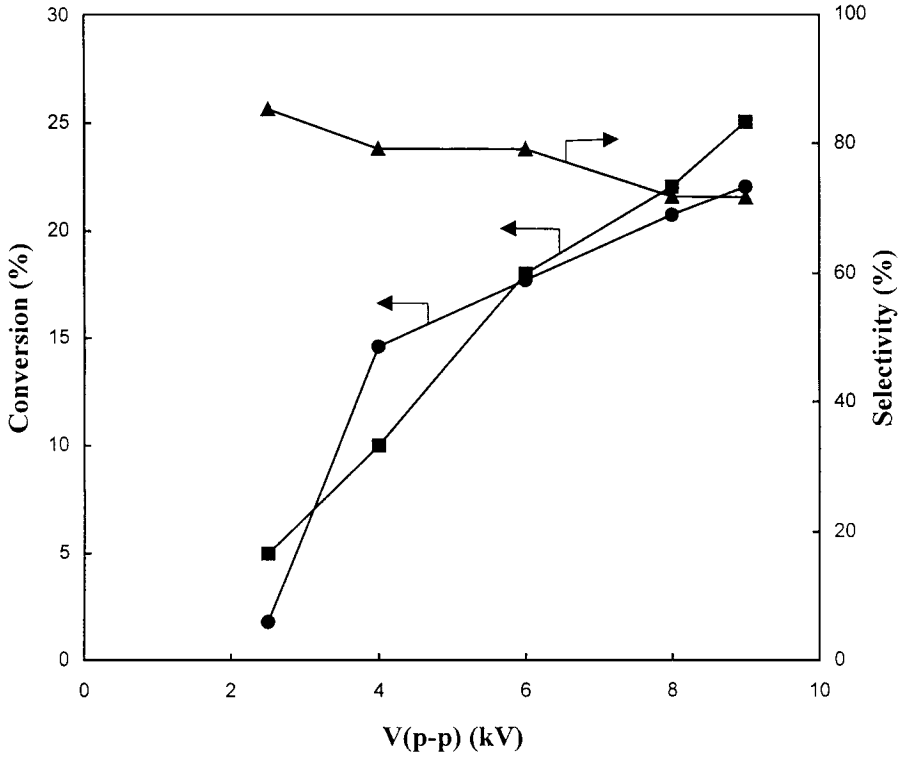


**FIG. 7.** Results of reactions between $CH_4$ and excited $CO_2$. (●) $CO_2$ conversion; (■) $CH_4$ conversion; (▲) CO selectivity; $CH_4/CO_2 = 1$; total flow rate = 40 ml/min.

### II. $CH_4 + CO_2$ Reactions by Micro-arc Plasmas

When the distance between the two inner electrodes in the different arms is shortened, micro-arc plasmas were observed in the junction area of the Y-type reactor when the input voltages were applied on both the $CH_4$ and $CO_2$ arms. Glow discharge plasmas were formed in the gaps between the inner electrodes and the inner walls of the quartz tubes. In addition to the appearance of a bright emission between two inner electrodes, a change in the current waveform was also observed. Spikes superimposed on the glow discharge in the current waveform indicate the formation of micro-arcs. No significant change was observed on the voltage waveform, but the maximum peak-to-peak current increased dramatically, as seen in Fig. 8. The study of the characteristic differences, such as electron temperature, electron and ion densities between normal glow discharge plasmas, and these micro-arcs, is still in progress. The results of the reactions at different $CH_4/CO_2$ ratios under these conditions are shown in Table 2.

Dependence of $CH_4$ and $CO_2$ conversions and selectivities of the products on the $CH_4/CO_2$ ratio with micro-arc formation shows a similar tendency to that of the reaction with only glow discharge plasmas. With an increasing $CH_4/CO_2$ ratio, the conversion of $CH_4$ and selectivities to hydrocarbons and hydrogen decreased while the conversion of $CO_2$ and selectivity to CO increased. Compared to glow discharge plasmas, micro-arc plasmas produced more CO and $H_2$ and smaller amounts of hydrocarbons. Micro-arc formation also improved the conversions of both $CH_4$ and $CO_2$.

## DISCUSSION

### I. Synergetic Effects and the Reaction Mechanism

The results of $CO_2$-reforming $CH_4$ reactions under different reaction conditions show that products from both partial oxidation of $CH_4$ and reduction of $CO_2$ were observed when both $CH_4$ and $CO_2$ plasmas were initiated.

**TABLE 2**

**Results of $CH_4 + CO_2$ Reaction with $CH_4$ and $CO_2$ Both Excited with Micro-arc Formation**

| $CH_4/CO_2$ (at.) | $X_{CH_4}$ (%) | $X_{CO_2}$ (%) | $S_{CO}$ (%) | $S_{C_2H_6}$ (%) | $S_{C_2H_4}$ (%) | $S_{C_2H_2}$ (%) | $S_{C_3H_8}$ (%) | $S_{H_2}$ (%) | $B_C$ (%) |
|---|---|---|---|---|---|---|---|---|---|
| 1/9 | 97.3 | 22.0 | 98.9 | 0.5 | 0.0 | 0.0 | 0.0 | 74.5 | 99.4 |
| 3/7 | 96.3 | 42.1 | 85.2 | 0.8 | 0.0 | 4.3 | 0.4 | 66.3 | 90.7 |
| 5/5 | 88.9 | 53.2 | 68.5 | 4.3 | 1.9 | 9.4 | 0.9 | 61.5 | 84.0 |
| 7/3 | 88.3 | 70.3 | 41.2 | 4.3 | 2.4 | 12.3 | 1.4 | 45.2 | 63.6 |
| 9/1 | 84.2 | 77.5 | 21.5 | 5.0 | 2.7 | 18.4 | 1.9 | 28.6 | 50.5 |

*Note.* $X_{CH_4}$ (%), conversion of $CH_4$; $X_{CO_2}$ (%), conversion of $CO_2$; $S_{CO}$ (%), selectivity of CO; $S_{C_2H_6}$ (%), selectivity of $C_2H_6$; $S_{C_2H_4}$ (%), selectivity of $C_2H_4$; $S_{H_2}$ (%), selectivity of $H_2$; $B_C$ (%), carbon balance.

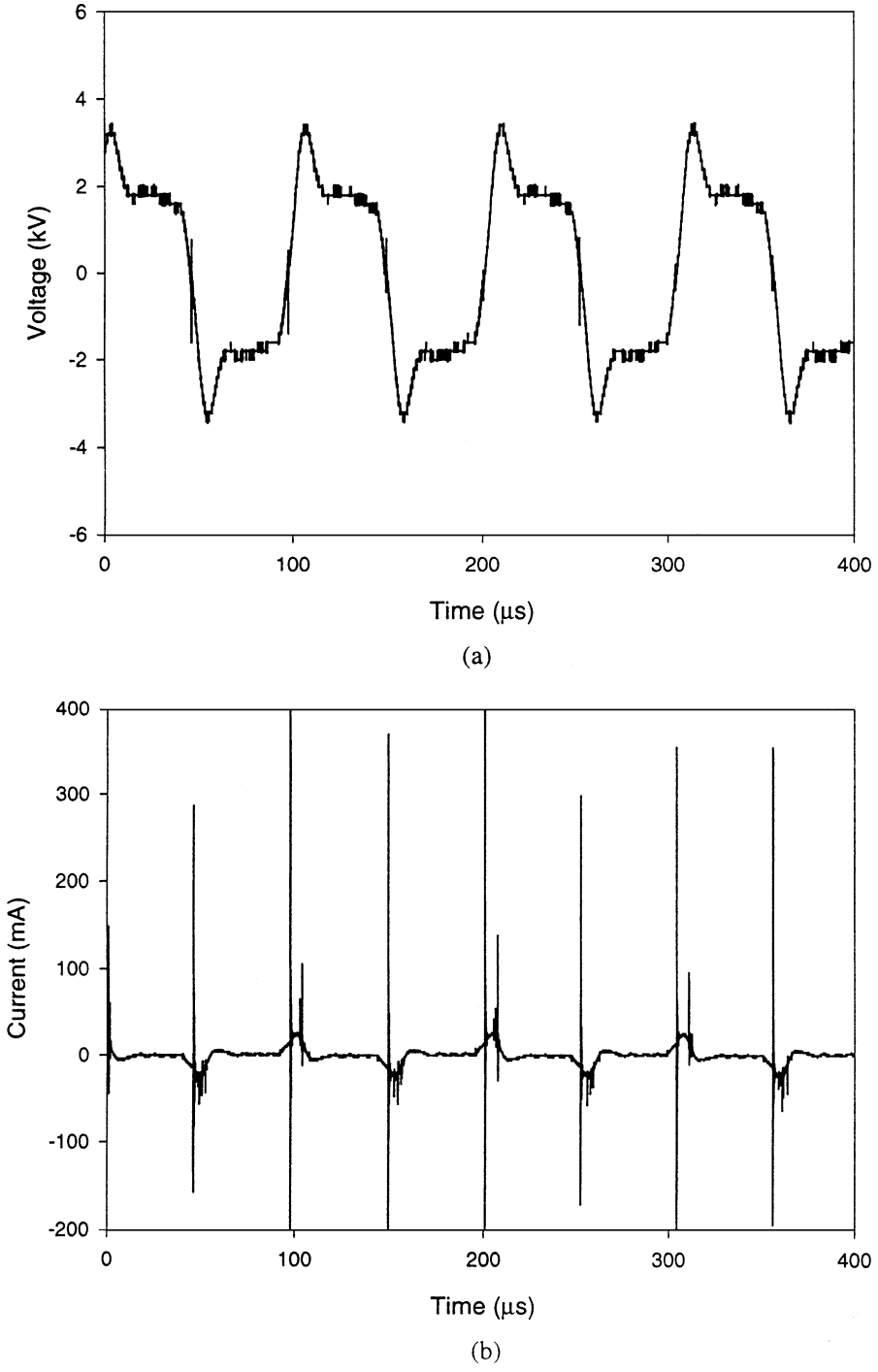


**FIG. 8.** Voltage (a) and current (b) waveforms for the reaction with micro-arc formation.

A comparison between total carbon-based CO selectivity, $S_{CO}$, and $CO_2$-based CO selectivity, ${}^*S_{CO}$, without the presence of a micro-arc, is shown in Table 3. At all $CH_4/CO_2$ ratios, ${}^*S_{CO}$ is much higher than $S_{CO}$, and also much higher than 100, which indicates a contribution from $CH_4$ to CO formation. A similar comparison when micro-arcs are formed during the reaction is shown in Table 4. A similar trend with respect to CO selectivity is observed, except that the contribution from $CH_4$ is even higher, indicating a higher degree of interaction between species in the two arms. Even without excitation of $CH_4$, partial oxidation of $CH_4$ by excited $CO_2$ occurred to produce CO as well as $C_2$'s and $C_3$'s. $CO_2$ conversion to CO was also observed in the reaction of $CO_2$ with excited $CH_4$, as shown in Figs. 6 and 7.

**TABLE 3**

**Comparison of Experimental Results with Theoretical Selectivities Assuming That No Reaction Occurs between $CH_4$ and $CO_2$**

| $CH_4/CO_2$ (at.) | $X_{CH_4}$ (%) | $X_{CO_2}$ (%) | $S_{CO}$ (%) | $^*S_{CO}$ (%) |
|---|---|---|---|---|
| 1/9 | 70.0 | 16.6 | 97.0 | 142 |
| 3/7 | 65.4 | 19.3 | 73.8 | 181 |
| 5/5 | 56.8 | 28.5 | 49.0 | 147 |
| 7/3 | 45.0 | 39.8 | 36.2 | 132 |
| 9/1 | 34.0 | 52.8 | 27.8 | 189 |

*Note.* $X_{CH_4}$ (%), conversion of $CH_4$; $X_{CO_2}$ (%), conversion of $CO_2$; $S_{CO}$ (%), selectivity of CO; $^*S_{CO}$, CO selectivity based on $CO_2$.

In addition to individual plasma reactions occurring in the different arms of the reactor, these results indicate that a synergetic effect was present between these reactions. This synergetic effect is due to interactions between species in the different arms. Due to the close proximity of the two inner electrodes, excited species from one arm may have a long enough lifetime to reach the junction area, where these species meet. For example, excited or unexcited species from one arm interact with species of the other arm to form products. Excited species such as CH in $CH_4$ plasmas (32) as well as excited O and $CO_2$ species in $CO_2$ plasmas (33, 34) have been observed in microwave plasma systems and glow discharge plasma systems. Therefore, a mechanism similar to that for surface reactions proposed by Bodrov and Apel'baum (35) is proposed as follows,

$$CH_4 + {}^* \rightarrow CH_4^* \rightarrow CH_3^* \rightarrow CH_2^* \rightarrow CH^* \rightarrow C^*, \quad [16]$$

$$CO_2 + {}^* \rightarrow CO_2^* \rightarrow CO + O^*, \quad [17]$$

$$CH_x^* + O^* \rightarrow CO + H_2 + 2^*, \quad [18]$$

$$C^* + O^* \rightarrow CO + 2^*, \quad [19]$$

$$CH_x^* \rightarrow C_2H_6, C_2H_4, C_2H_2, C_3H_6, \quad [20]$$

$$CH_x^* + CO_2 \rightarrow CO + x/2H_2 + {}^*, \quad [21]$$

$$CH_4 + O^* \rightarrow CO + 2H_2 + {}^*, \quad [22]$$

where an asterisk represents an activated species.

**TABLE 4**

**Reactions of $CO_2$-Reforming $CH_4$ with Micro-arc Formation**

| $CH_4/CO_2$ (at.) | $X_{CH_4}$ (%) | $X_{CO_2}$ (%) | $S_{CO}$ (%) | $^*S_{CO}$ (%) |
|---|---|---|---|---|
| 1/9 | 97.3 | 22.0 | 98.9 | 148 |
| 3/7 | 96.3 | 42.1 | 85.2 | 169 |
| 5/5 | 88.9 | 53.2 | 68.5 | 183 |
| 7/3 | 88.3 | 70.3 | 41.2 | 162 |
| 9/1 | 84.2 | 77.5 | 21.5 | 232 |

*Note.* $X_{CH_4}$ (%), conversion of $CH_4$; $X_{CO_2}$ (%), conversion of $CO_2$; $S_{CO}$ (%), selectivity of CO; $^*S_{CO}$, CO selectivity based on $CO_2$.

In the $CH_4$ arm, when an input voltage was applied, $CH_4$ was excited to its excited state, $CH_4^*$, which can further break down into $CH_3^*$, $CH_2^*$, $CH^*$, and $C^*$ along the reactor tube. The area closer to the junction will have higher $C^*$ concentration because of the longer retention time, which enables further breakdown of $CH_x^*$ to $C^*$. Due to the closeness of the ends of the two inner electrodes, $C^*$ can reach the junction area to react with $O^*$ species generated from the $CO_2$ arm to form CO. Some $CH_x^*$ might also reach the junction area to form $C_2$'s and $C_3$'s, or react with $O^*$ to form CO and $H_2$ before being further broken down into $C^*$.

In the case when only $CH_4$ was excited, $CH_x^*$ can react with $CO_2$ to form CO and $H_2$ as shown in Eq. [21]. Equations [17] and [21] may represent the reactions that occur when only $CO_2$ was excited.

With micro-arc formation, because the inner electrodes are even closer, the time for the species from the $CH_4$ arm to reach the junction area was shorter, which enabled more species to have enough time to reach the junction area to meet $O^*$ produced from $CO_2$ activation. The higher energy of micro-arc plasmas also favored the formation of deep breakdown species such as $C^*$. The formation of micro-arcs in the junction area might have further broken down $CH_x^*$ to $C^*$ at the junction, which favored CO formation; therefore, this can cause an increase in the selectivity to CO in these reactions.

## II. Energy Efficiencies

The energy efficiencies for the reactions between excited $CO_2$ and excited $CH_4$ with and without formation of micro-arcs at different $CH_4/CO_2$ ratios are shown in Fig. 9. The energy efficiencies (efficiency of converting electric energy to chemical energy) are calculated using Eqs. [10]–[12]. The

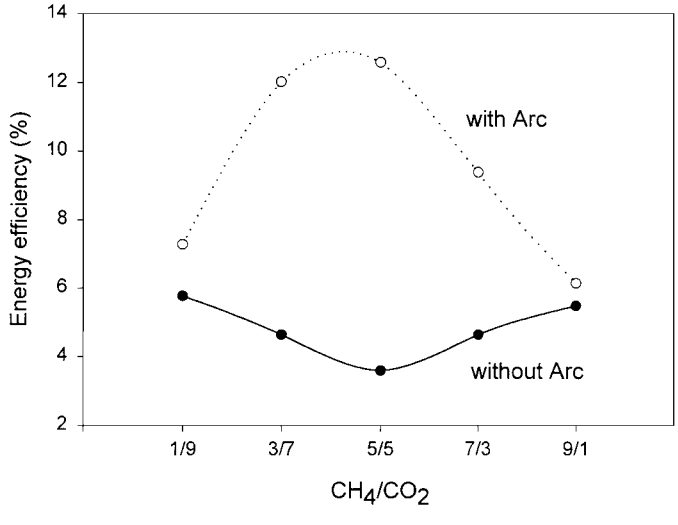


**FIG. 9.** Dependence of energy efficiencies on $CH_4/CO_2$. $V_{rms} = 2.10$ kV; $I_{rms} = 17.4$ mA.

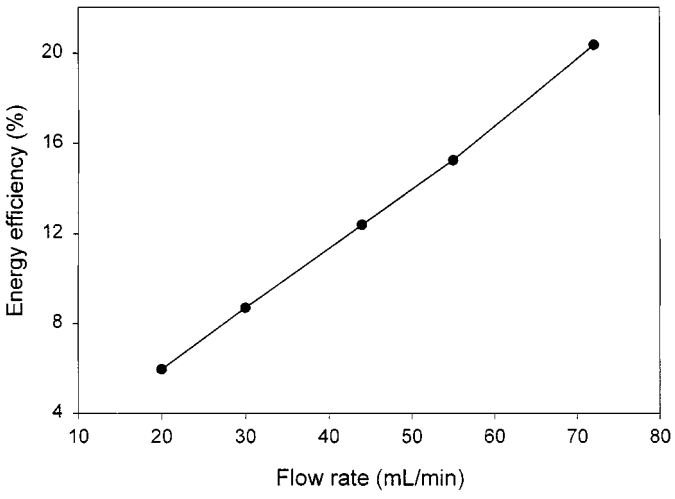


**FIG. 10.** Dependence of energy efficiency on the flow rate. $V_{rms} = 2.10$ kV; $I_{rms} = 17.4$ mA.

heat of formation of coke in the reactions is excluded in the calculations. The energy efficiencies, $\xi$, for the reactions without micro-arc formation are in the range of 4.6–7.4%. As the $CH_4/CO_2$ ratio increases, $\xi$ decreases initially and then increases as $CH_4/CO_2$ further increases. $\xi$ reaches a minimum at $CH_4/CO_2 = 1$. On the contrary, with micro-arc formation, $\xi$ increased with increasing $CH_4/CO_2$, maximized at $CH_4/CO_2 = 1$, and then decreased with a further increase of $CH_4/CO_2$. With micro-arc formation, the energy efficiencies were higher than those without micro-arcs. This is due to the formation of a larger amount of CO, which has a higher heat of formation than hydrocarbons. The maximum energy efficiency reached about 16% at $CH_4/CO_2 = 1$ with the presence of micro-arcs.

The dependence of energy efficiencies on reaction flow rates is shown in Fig. 10. Increasing the flow rate increased the energy efficiency, although the conversions of both reactants decreased because the total amount of reactants converted increased and the reaction rate increased as the flow rate increased.

The maximum energy efficiency observed, in terms of energy used to convert $CH_4$ and $CO_2$ to CO, represented in the unit of J/L of CO, can be calculated as follows,

$$\frac{E_{\text{exp}}(\text{J/s})}{0.0750(\text{L/min}) \times (1\ \text{min}/60\ \text{s}) \times 10\% \times 70\%} = 343\ \text{kJ/L of CO},$$

where $E_{\text{exp}}$ is 30 J/s calculated according to Eq. [12].

For an approximate comparison of energy efficiency between this plasma process and conventional catalytic processes, the energy efficiency of catalytic processes is calculated based on the thermodynamic data of the reaction. The energy for CO formation according to the following reaction is 5.5 kJ/L of CO.

$$CH_4 + CO_2 \rightarrow 2CO + 2H_2,\ \Delta H^{\circ}_{298K} = 247.0\ \text{kJ/mol}.$$

Although the plasma approach operates at room temperature, which is an advantage over conventional methods, it has a much lower energy efficiency in $CO_2$ reforming of $CH_4$ to CO compared to conventional thermal catalytic processes. Therefore, a large energy efficiency gap still needs to be filled for the plasma process to become a competitive alternative to conventional catalytic methods.

## CONCLUSIONS

$CO_2$-reforming $CH_4$ reactions by glow discharge plasmas with and without micro-arc formation using a Y-type reactor were studied. The process is effective in converting $CH_4$ and $CO_2$ into CO and $H_2$. The reaction products included CO, $H_2$, and a small amount of hydrocarbons. Interactions between species from different arms are suggested based on the product distributions and the comparison between total-carbon-based CO selectivity and $CO_2$-based CO selectivity. This interaction was also observed when only one reactant was excited. Reactions with the formation of micro-arcs produced more CO as well as higher energy efficiencies than those without micro-arc formation. Compared with conventional catalytic methods, this plasma approach has lower energy efficiency in CO formation from $CO_2$ reforming of $CH_4$.

## ACKNOWLEDGMENTS

Dr. Stephanie L. Brock and Jeffery Rozak are acknowledged for helpful discussions. This research was supported by Fujitsu Ltd., Honda Research and Development, and Hokushin Co.

## REFERENCES

1. Akimoto, H., and Narita, H., Atm. Environ. (Oxford, England) **28**, 213 (1994).
2. Treece, J., Automotive News 3 Feb 23 (1998).
3. Manahan, S., "Environmental Chemistry," 6th ed., p. 338. Lewis Publishers: Boca Raton, FL, 1994.
4. Meehl, G. A., and Washington, W. M., *Nature* **382**, 56 (1996).
5. Sellers, P. J., Bounoua, L., Collatz, G. J., Randall, D. A., Dazlich, D. A., Los, S. O., Berry, J. A., Fung, I., Tucker, C. J., Field, C. B., and Jensen, T. G., *Science* **271**, 1402 (1996).
6. Edwards, J. H., *Catal. Today* **23**, 59 (1995).
7. Knutson, T. R., Tuleya, R. E., and Kurihara, Y., *Science* **279**, 1018 (1998).
8. McKibben, W., *Audubon* **100** (March–April), 54 (1998).
9. Hileman, B., *Chem. Eng. News* **75**, 30 (1997).
10. Sheahen, T. P., *Natl. Rev.* **49**, 31 (1997).
11. Dibby, D. M., Chang, C., Howe, R. F., and Yurchak, S., "Studies Surface Science Catalysis," Vol. 36. Elsevier, Amsterdam, 1988.
12. Mark, M. F., and Maier, W. F., *J. Catal.* **164**, 122 (1996).
13. Ayers, W. M., Ed., "Catalytic Activation of Carbon Dioxide," ACS Symposium Series 363. American Chemical Society, Washington, DC, 1988.

14. Azar, C., and Rodhe, H., *Science* **276**, 1818 (1997).
15. Kurz, G., and Teuner, S., *Erdol. Kohle.* **43**, 171 (1990).
16. Van den Oosterkamp, P. F., Chen, Q., Overwater, J. A. S., Ross, J. R. H., and van Keulen, A. N. J., *in* "Meeting of Large Chemical Plants, Antwerp, Belgium, Oct. 1995." The Royal Flemish Society of Engineers.
17. Van Keulen, A. N. J., Seshan, K., and Hobink, J. H. B. J., *J. Catal.* **166**, 306 (1997).
18. Bitter, J. H., Seshan, K., and Lercher, J. A., *J. Catal.* **176**, 93 (1998).
19. Bradford, M. C. J., and Vannice, M. A., *J. Catal.* **173**, 157 (1998).
20. Dissanayake, D., Rosynek, M. P., Kharas, K. C. C., and Lunsford, J. H., *J. Catal.* **132**, 117 (1991).
21. Theron, J. N., Fletcher, J. C. Q., and O'Connor, C. T., *Catal. Today* **21**, 489 (1994).
22. Choudhary, V. R., Rajput, A. M., and Rane, V. H., *J. Phys. Chem.* **96**, 8686 (1992).
23. Kim, G. J., Cho, D. S., Kwang, H., and Kim, J. H., *Catal. Lett.* **28**, 41 (1993).
24. Choudhary, V. R., Uphade, B. S., and Mamman, A. S., *Microporous Mesoporous Mater.* **23**, 61 (1998).
25. Bradford, M. C. J., and Vannice, M. A., *Catal. Rev.-Sci. Eng.* **41**, 1 (1999).
26. Cenian, A., Chernukho, A., Borodin, V., and Sliwinski, G., *Contib. Plasma Phys.* **34**, 25 (1994).
27. Huang, J., and Suib, S. L., *J. Phys. Chem.* **97**, 9403 (1993).
28. Marun, C., Suib, S. L., Dery, M., Harrison, J. B., and Kablaoui, M. J., *J. Phys. Chem.* **100**, 17866 (1996).
29. Futamura, S., and Yamamoto, T., *IEEE Trans. Ind. Appl.* **33**, 447 (1997).
30. Hsiao, M. C., Merritt, B. T., Vogtlin, J. J., and Kushner, M. J., *J. Appl. Phys.* **74**, 5378 (1993).
31. Xia, G., Huang, A., Wang, J., and Suib, S. L., in preparation.
32. De la Cal, E., Tafalla, D., and Tabares, F. L., *J. Appl. Phys.* **73**, 948 (1993).
33. Suib, S. L., Brock, S. L., Marquez, M., Luo, J., Matsumoto, H., and Hayashi, Y., *J. Phys. Chem. B* **102**, 9661 (1998).
34. Sim, W., and Haugh, M., *J. Chem. Phys.* **65**, 1616 (1976).
35. Bodrov, I. M., and Apel'baum, L. O., *Kinet. Katal.* **8**, 379 (1967).